22. A. J. Parker, *Chem. Rev.* **69**, 1 (1969).
23. K. W. Y. Abell and A. J. Kirby, *Tetrahedron Lett.* **27**, 1085 (1986).
24. Supported in part by Faculty Research Award FRA369 from the American Cancer Society and by grant GM38273 from the National Institutes of Health (to D.H.), a fellowship from the Jane Coffin Childs Memorial Fund for Medical Research (to C.L.), and a fellowship from the Verband der Chemischen Industrie (to T.K.). We gratefully acknowledge the assistance of S. Miller for preliminary experiments, J. Patel for constructive suggestions, and C. Grimshaw and D. Goodin for helpful discussions about the kinetic analyses of tight-binding inhibitors.

16 April 1991; accepted 19 June 1991

Differential Phosphorylation of the Transcription Factor Oct1 During the Cell Cycle

SUSAN BOSEMAN ROBERTS, NEIL SEGIL, NATHANIEL HEINTZ

Orderly progression through the somatic cell division cycle is accompanied by phase-specific transcription of a variety of different genes. During S phase, transcription of mammalian histone H2B genes requires a specific promoter element and its cognate transcription factor Oct1 (OTF1). A possible mechanism for regulating histone H2B transcription during the cell cycle is direct modulation of Oct1 activity by phase-specific posttranslational modifications. Analysis of Oct1 during progression through the cell cycle revealed a complex temporal program of phosphorylation. A $p34^{cdc2}$-related protein kinase that is active during mitosis may be responsible for one mitotic phosphorylation of Oct1. However, the temporally controlled appearance of Oct1 phosphopeptides suggests the involvement of multiple kinases and phosphatases. These results support the idea that cell cycle–regulated transcription factors may be direct substrates for phase-specific regulatory enzymes.

CYCLING EUKARYOTIC CELLS ALTERnate between mitosis (M phase) and DNA replication (S phase) through an orderly progression of biochemical processes. An example of the maintenance and control of this order is the close coupling of histone gene transcription and the onset of chromosomal DNA synthesis (*1*). In mammalian cells, coordinate induction of the five families of histone genes during S phase is not a result of activation of a single transcription factor, but is achieved through distinct factors that interact with subtype-specific promoter elements (*2–5*). This suggests the existence of a pleiotropic mechanism for regulating the activity of transacting factors with specific functions in S phase of the cell cycle (*4*). A single mechanism with diverse molecular targets might be fundamental to the control of S phase, perhaps regulating factors involved in processes as diverse as transcription and DNA replication.

The transcription factor Oct1 (OTF1) has been implicated in transcriptional activation of a variety of genes (*5, 6*) including the genes encoding histone H2b (*5, 7*). Oct1 stimulates H2b transcription in vitro through its interaction with a sequence that contains the octamer motif (ATTTGCAT), which is evolutionarily conserved in histone H2b genes at a precise position adjacent to the TATA box (*8*). S phase–specific activation of histone H2b genes in vivo and in vitro requires this subtype-specific promoter element (*4, 5*). Oct1 can also stimulate initiation of adenovirus DNA replication in vitro (*9*), raising the possibility that Oct1 may also be involved in chromosomal DNA synthesis. These studies suggest that the activity of Oct1 or an associated protein is modulated in a cell cycle–dependent manner and implicate Oct1 as a target of a general cell cycle regulatory mechanism.

Phosphorylation and dephosphorylation are known to alter nuclear protein activities and interactions at specific phases of cell cycle. For example, both the G2 to M and G1 to S cell cycle transitions are dependent on the activity of cdc2 protein kinase (*10*), which is regulated by specific phosphorylations and dephosphorylations (*11*). Furthermore, phosphorylation of Oct1 in vivo has been demonstrated by transfection of Oct1 constructs into HeLa cells (*12*). We analyzed the phosphorylation state of Oct1 in actively cycling mammalian cells to determine whether differential phosphorylation of Oct1 is correlated with its ability to activate transcription of the H2B gene during the cell cycle.

Polyclonal antiserum to Oct1 (anti-Oct1) (*13*) was used to analyze Oct1 from whole cell extracts prepared from synchronously growing HeLa cells. There was no change in the abundance (Fig. 1B) or rate of synthesis (Fig. 1C) of Oct1 during the cell cycle except in cells arrested in mitosis (Fig. 1C, lane N), where synthesis of Oct1 as well as lamin B (control) was depressed. Synchronized cells were labeled for one hour (pulse-labeled) with [^{32}P]orthophosphate; immunoprecipitation with anti-Oct1 of whole cell extracts produced a pattern of protein bands that migrated in the position expected for Oct1, but that was more complex than the pattern seen by immunoblot analysis (Fig. 1B) or from immunoprecipitates of [^{35}S]methionine-labeled Oct1 (Fig. 1C). The most obvious difference in the Oct1 pattern was from cells blocked in mitosis by nocodazole (N) where there was a dramatic increase in ^{32}P incorporation and a retarded migration. The retarded migration of Oct1 from cells blocked in mitosis was also apparent in the immunoblot (Fig. 1B, lane N) and the [^{35}S]methionine-labeled sample (Fig. 1C, lane N*). In addition to the difference in M phase, there was a difference in the pattern of ^{32}P-labeled Oct1 bands from cells in S phase (+4 and +8 hours) compared to the pattern from cells in G1 and G2+M (G1, +12, +16, +20 hours) or cells blocked at the G1 to S boundary by aphidicolin (A). The middle band was absent in S phase (+4 and +8). The fluorescence-activated cell sorting (FACS) analysis (Fig. 1A) and the pattern of [^{32}P]orthophosphate incorporation into lamin B (Fig. 1D) (*14*) establish that the method used for analysis of the synchronized whole cell extracts is reliable and stage-specific.

The change in Oct1 at mitosis was detected by one-dimensional gel electrophoresis because of the massive increase in ^{32}P-incorporation in nocodazole-blocked cells (N), but variability of the method for resolving differences in Oct1 during interphase prompted the use of two-dimensional gel fractionations. Two-dimensional gel analysis of Oct1 chromatographically purified from logarithmically growing cells (Fig. 2A) indicated that Oct1 can be resolved on the basis of charge into five species and that the different forms of Oct1 are detected by anti-Oct1. Immunoprecipitates of ^{32}P-labeled Oct1 from synchronized cells were also fractionated by two-dimensional gel electrophoresis (Fig. 2B). G1 phase cells (Fig. 2B, panel G1) contained five species of Oct1 that were very similar to the pattern of purified protein (Fig. 2A). The relative labeling of the Oct1 species changed in cells arrested at the G1 to S boundary by aphidicolin (Fig. 2B, panel G1a). The ^{32}P-labeled Oct1 species immunoprecipitated from S phase cells (panel S) differed in relative labeling and migration from those in G1. The labeled Oct1 species from S phase were shifted toward the basic end of the isoelec-

Howard Hughes Medical Institute, Laboratory of Molecular Biology, Rockefeller University, 1230 York Avenue, New York, NY 10021.

tric focusing (IEF) gradient, consistent with labeling of more positively charged molecules. The species of ^{32}P-labeled Oct1 from mitotic cells (Fig. 2B, panel M) were shifted dramatically toward the acidic end of the IEF gradient, consistent with the labeling of more negatively charged species. The two-dimensional analysis did not distinguish among the possible modifications that could change the charge of Oct1. The two-dimensional gel patterns are consistent with the one-dimensional analysis (Fig. 1D) that suggested a difference in Oct1 between G1 and S phase and demonstrated that Oct1 is hyperphosphorylated during mitosis.

To determine whether the shifts in charge of Oct1 were a result of changes in phosphorylation and to confirm that additional sites were phosphorylated during mitosis, two-dimensional tryptic phosphopeptide maps of immunoprecipitated ^{32}P-labeled Oct1 were prepared. The complex patterns of ten tryptic phosphopeptides (Fig. 3A) changed at specific stages of the cell cycle. Two distinct interphase peptides (6 and 10) were visible in the maps from G1 and S phase cells. Three additional phosphopeptides (1, 2, and 4) were present, but the intensity of the spots was less than the intensity of 6 and 10. As cells entered G2 (S/G2), peptides 1, 2, and 4 became more prominent, and three new peptides, 3, 8, and 9, appeared. The population that contained mitotic cells (G2/M/G1) had two additional phosphopeptides (5 and 7); all ten of the phosphopeptides analyzed were present in this population of cells.

The intensity of the phosphopeptides (1 to 10) did not change coordinately as HeLa cells progressed toward division. Specifically, peptides 3, 8, and 9 appeared before 5 and 7; peptides 1, 2, and 4 were present at all times. These differences suggest that a complex program of phosphorylation regulates Oct1 activity as cells progress through G2 and mitosis. The pulse-labeling protocol used in this experiment would not reveal differences in phosphates added during G2+M and removed in G1 or S phase. The pattern of Oct1 phosphorylation in G1 (Fig. 3A) and the electrophoretic mobilities of Oct1 from G1 compared to those in mitosis (Fig. 2B, panels G1 and M) demonstrated that most of the hyperphosphorylation of Oct1 in G2+M was reversed in G1; however, the rate of disappearance of ^{32}P from Oct1 in cells labeled during mitosis and analyzed during G1 (*15*) supported the idea that some mitotic phosphates persist through G1.

To determine which peptides are phosphorylated by enzymes active during mitosis, we analyzed phosphopeptides from cells blocked in mitosis by nocodazole (Fig. 3A, M). Cells blocked in mitosis (M) contained six equally labeled phosphopeptides (2, 3, 5, 7, 8, and 9), but the two major (6 and 10) and two minor (1 and 4) interphase (G1, S, and G2) phosphopeptides were absent. The presence of the mitotic phosphopeptides in the cycling population (G2/M/G1) shows that the hyperphosphorylation seen in nocodazole-blocked cells is a reflection of the mitotic state and not an artifact caused by drug synchronization. Thus, there is a qualitative difference in Oct1 phosphorylation in mitotic compared to interphase cells. We do not know if the interphase-specific phosphopeptides (6 and 10) disappear because additional modifications take place or if the phosphorylation sites on interphase peptides are not phosphorylated during mitosis.

Results of the phosphopeptide analyses from cycling cells and cells blocked in mitosis suggested that mitotic phosphorylation of Oct1 may result from several different enzymes that are active during mitosis. Different enzyme activities could lead to the different time of appearance of the various phosphopeptides. Phosphoamino acid analysis (Fig. 3B) supported this hypothesis, showing that interphase phosphorylation of Oct1 occurred exclusively on serine, whereas mitotic Oct1 is extensively labeled on threonine and serine. The appearance of phosphothreonine in Oct1 from cells blocked in mitosis suggests that peptides 5 and 7, the last ^{32}P-labeled phosphopeptides to appear in the cell cycle analysis, are phosphorylated on threonine. The temporal pattern of phosphorylation suggests that Oct1 could be a useful substrate for determining the order of changing kinase and phosphatase activities as cells enter mitosis.

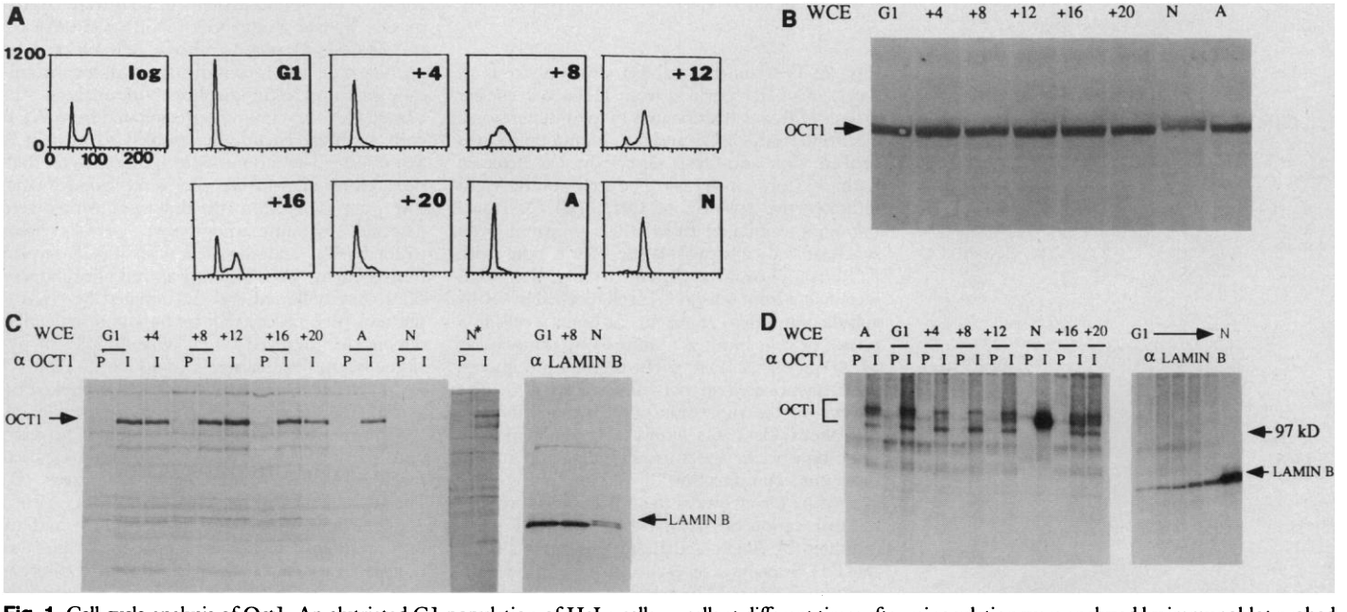

Fig. 1. Cell cycle analysis of Oct1. An elutriated G1 population of HeLa cells was inoculated into fresh medium and allowed to progress synchronously through the cell cycle. Aliquots were removed at 4-hour intervals for analysis (*21*). (**A**) FACS analysis. Histograms (abscissa, relative fluorescence; ordinate, cell number) show the relative DNA content of logarithmically growing HeLa cells (log), the G1 population progressing through the cell cycle (G1, +4, +8, +12, +16, +20), G1 cells blocked by aphidicolin (A) (*22*), and mitotic cells blocked by nocodazole (N) (*23*). (**B**) Whole cell extracts (WCE) made from cells at different times after reinoculation were analyzed by immunoblot probed with anti-Oct1. WCE pulse-labeled for 1 hour with (**C**) [^{35}S]methionine or (**D**) [^{32}P]orthophosphate were immunoprecipitated with Oct1 (I), preimmune (P), or lamin B antisera and protein A Sepharose (*24*). The immunoprecipitates were fractionated by 7.5% SDS–polyacrylamide gel electrophoresis (PAGE) (*25*). Lane N* is a long exposure of lane N. The arrow (→) represents +4, +8, +12, and +16. The labeled bands were detected by either fluorography (C) or autoradiography (D).

Hyperphosphorylation of Oct1 during mitosis suggested that Oct1 may be a substrate for $p34^{cdc2}$ protein kinase. This hypothesis is supported by the existence of a consensus site for phosphorylation by $p34^{cdc2}$ in the deduced amino acid sequence of Oct1 (*16*); therefore, we determined whether Oct1 could be phosphorylated by $p34^{cdc2}$ mitotic kinase. Sepharose beads bound to the protein $p13^{suc1}$ (*17*), which interacts with $p34^{cdc2}$ and related kinases, were used to isolate cdc2 protein kinases from synchronized HeLa cells. The preparations were assayed with histone H1 as a substrate for these activities in cell cycle extracts. Oct1 was included in the experiments, but phosphorylation was below the level of detection relative to H1 and an endogenous 105-kD mitotic substrate, which was two to four times more abundant than Oct1 (*15*). Higher concentrations of p13-associated kinase from maximally activated M phase extracts phosphorylated Oct1 (Fig. 4A). The ^{32}P-labeled Oct1 phosphorylated by the p13-associated mitotic kinase was digested with trypsin for two-dimensional peptide mapping. Mixing of tryptic phosphopeptides (Fig. 4B, panel 3) from Oct1 labeled in vivo during mitosis (Fig. 4B, panel 2) with Oct1 labeled in vitro with p13-associated kinase (Fig. 4B, panel 1) showed that one of the six mitotic peptides that was labeled in vivo (Fig. 3A, peptide 3) comigrated with a phosphopeptide that was also labeled in vitro. Comigration of the phosphopeptides was confirmed by analyzing thermolysin digests (*15*).

The high affinity and specificity of p13 beads for $p34^{cdc2}$ and related mitotic kinases (*17*) and the appearance of peptide 3 (Fig. 3A, S/G2) late in the cell cycle support a direct role for a $p34^{cdc2}$-related mitotic kinase that modifies Oct1 in vivo. However, five of the six phosphopeptides detected in mitotic cells in vivo are probably not the result of p13-associated kinase activity, supporting our hypothesis that other kinases also phosphorylate Oct1.

The modifications of Oct1 as cells progress through the division cycle suggest that histone H2B transcription may be regulated by direct modulation of Oct1 transcriptional activity. As cells exit S phase and histone H2B transcription returns to a constitutive octamer-independent mode, phosphorylation of Oct1 phosphopeptides 3, 8, and 9 was observed. Because peptide 3 was phosphorylated in vitro by a p13-associated mi-

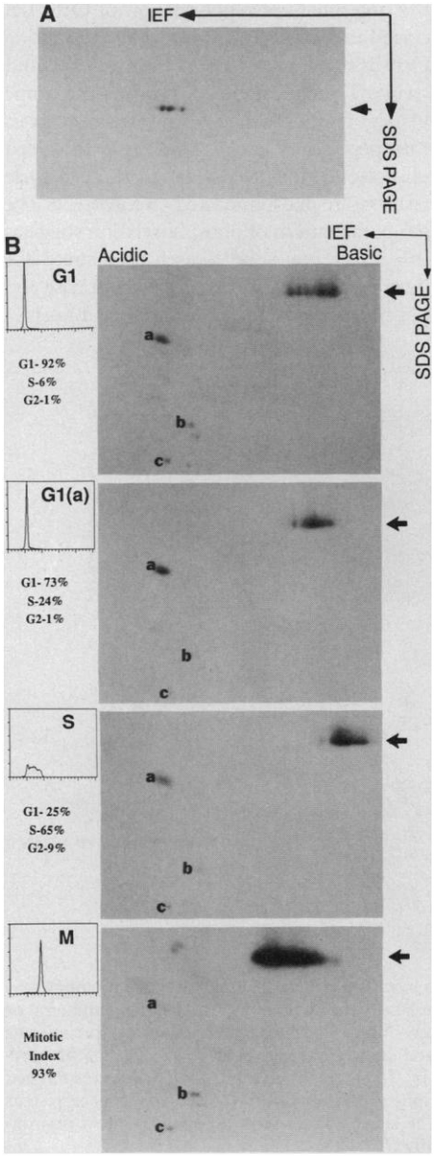

Fig. 2. Two-dimensional gel electrophoresis of Oct1. (**A**) Oct1 purified from HeLa cell nuclear extract (*13*) was fractionated by two-dimensional electrophoresis (*25*), and an immunoblot was probed with anti-Oct1. Antibody was detected with [^{125}I]protein A (*24*). The arrow on the right indicates the position of Oct1. (**B**) Oct1 was immunoprecipitated from WCE prepared from synchronized cells pulse-labeled for 1 hour with [^{32}P]orthophosphate (legend to Fig. 1). WCE were made from cells in G1; cell blocked in G1 by aphidicolin, G1(a) (5 μg/ml, 12 hours); cells in S phase; or cells blocked in mitosis by nocodazole, M (40 ng/ml, 12 hours). The immunoprecipitates were fractionated in two dimensions (*26*). The arrows on the right side of each panel indicate ^{32}P-labeled Oct1. The letters (a, b, and c) indicate three nonspecific spots used to align the autoradiograms. The direction of electrophoresis is indicated by the arrows at the top of the figure, and the orientation of the first-dimension IEF gel is indicated by Acidic and Basic. Histograms show the FACS analysis of each cell population, analyzed as in Fig. 1. The numbers (%) below each histogram are an estimate of the distribution of cells at various stages of the cell cycle in each population. A reagent for cleaner immunoprecipitations was made by chemically coupling rabbit Oct1 antibody to protein A–Sepharose beads (Pierce). Covalent coupling prevents release of immunoglobulin and subsequent overload of polyacrylamide gels.

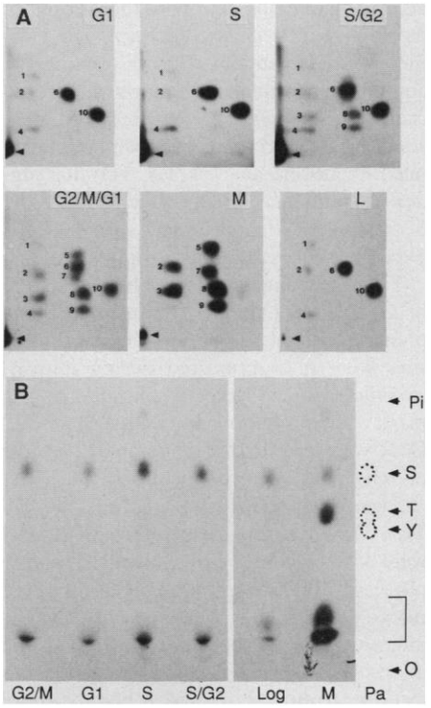

Fig. 3. Tryptic phosphopeptide and phosphoamino acid analysis of Oct1 labeled in vivo at various times of the cell cycle. Oct1 was immunoprecipitated from WCE prepared from synchronized HeLa cells (legend to Fig. 1) labeled for 1 hour with [^{32}P]orthophosphate. The cells were labeled in G1, S, late S and G2 (S/G2), G2+M+G1 (G2/M/G1), M phase (mitotic cells blocked by nocodazole), and L (unsynchronized, logarithmically growing). (**A**) Phosphopeptide analysis. ^{32}P-labeled Oct1 was immunoprecipitated from WCE with antibody chemically coupled to protein A Sepharose. The immunoprecipitates were fractionated by SDS-PAGE (7.5% acrylamide) (*25*). The Oct1 bands from the dried gel, which were detected by autoradiography, were excised, washed (*27*), and digested with TPCK-trypsin (Calbiochem) (*28*). The trypsinized phosphopeptides were collected and fractionated by electrophoresis (pH 3.5, cathode on the right) in the first dimension, followed by chromatography in pyridine:butanol:water:acetic acid [15:10:12:3 (v/v)] (*27*). The origin of each sample is marked by a triangle. All samples were run in parallel. A specific number was assigned arbitrarily to each spot. Each panel is from an autoradiogram exposed for 10 to 14 days with an intensifying screen. (**B**) Phosphoamino acid analysis. An aliquot of each sample was hydrolyzed in HCl (6 N) (*27*), and the phosphoamino acids were applied to thin-layer cellulose plates and fractionated by electrophoresis (pH 1.9). Unlabeled phosphoamino acid markers [phosphoserine, S (20 μg); phosphothreonine, T (20 μg); phosphotyrosine, Y (20 μg)] were added to each sample and visualized with ninhydrin. Pa, phosphoamino acid standards; O, the position where the samples were loaded; Pi, the migration of labeled inorganic phosphate liberated during hydrolysis. The bracket indicates the position of unhydrolyzed phosphopeptides.

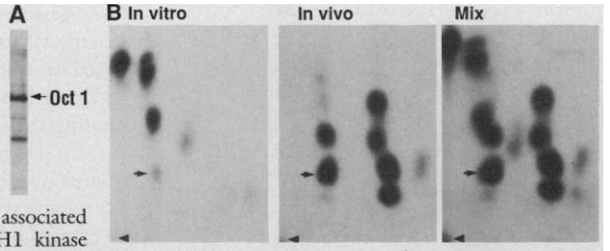

Fig. 4. Phosphorylation of Oct1 by $p13^{suc1}$-associated cdc2 protein kinase. (**A**) $p13^{suc1}$ beads were used to affinity-purify cdc2 protein kinase from cell cycle extracts. Kinase activity from each extract was assayed by phosphorylation of histone H1 (*29, 30*). No kinase activity was associated with mock beads. Increasing H1 kinase activity indicative of cdc2 protein kinase activation was associated with $p13^{suc1}$ beads incubated with WCE from progressively later stages in the cell cycle. A phosphorylation reaction was carried out with the fully activated kinase and purified Oct1 protein. Washed beads were incubated with 50 to 100 ng of Oct1 in kinase buffer and γ-[^{32}P]ATP (0.3 μM, 6000 Ci/mmol) in a 100-μl reaction for 30 min. The p13 beads and associated proteins were removed from the reactions prior to addition of Laemmli sample buffer to the supernatant. Phosphorylated Oct1 is indicated with an arrow. (**B**) The in vitro–phosphorylated Oct1 band indicated in Fig. 4A was excised and digested with trypsin, and phosphopeptides were separated in two dimensions as described in Fig. 3. Oct1 from in vivo–labeled cells was prepared as in Fig. 3 (M). Approximately twice as many counts per minute of peptides labeled in vivo were mixed with peptides labeled in vitro for the mixing experiment. Arrows indicate an in vitro–phosphorylated peptide that comigrated in the mixing experiment with peptide 3 from in vivo–labeled Oct1.

totic kinase (Fig. 4B), it is possible the decrease in H2B transcription at the end of S phase results from direct modification of Oct1 by a cell cycle–regulated protein kinase. The appearance of peptides 5 and 7 late in the progression experiment and in cells blocked in mitosis, coupled with the absence of the major interphase phosphopeptides 6 and 10 in mitotic cells demonstrate that progression from G2 to M phase is accompanied by further modification of Oct1. Although transcription of H2B genes has already returned to a basal level by this time in the cell cycle, hyperphosphorylation of Oct1 at mitosis probably results in complete loss of functional activity. This is consistent with our observation of a dramatic decrease in the specific activity of Oct1 DNA binding in whole cell extracts prepared from mitotic cells (*13*). Entry into G1 results in removal of most of the mitotic phosphates from Oct1 (Figs. 2B and 3A). We propose that loss of mitotic phosphorylations from Oct1 upon entry into G1 restores Oct1 DNA binding and basal Oct1 function. Finally, as cells progress from G1 to S the migration of Oct1 during gel electrophoresis was altered; this correlates with activation of Oct1-dependent transcription of the H2B gene. However, we have not identified a specific post-translational modification to explain the observed differences. Activation of Oct1-dependent H2B transcription in S phase may require removal of inhibitory phosphates transferred to Oct1 during mitosis, as observed for SV40 T antigen regulation of DNA replication (*18*). Activity of T antigen is dependent on phosphorylation by cdc2 protein kinase (*19*) and removal of inhibitory phosphates by protein phosphatase 2A, which is preferentially active in S phase nuclear extracts (*20*). Analysis of Oct1 dephosphorylation as cells enter G1 phase has demonstrated that some phosphorylations persist for many hours after release from a nocodazole block, but difficulties in achieving a synchronous exit from the nocodazole block have precluded a definitive test of this idea (*15*).

These results suggest that cell cycle–regulated transcription factors may be substrates for enzymes that perform key functions in the somatic cell cycle. Identification of the enzymes responsible for modification of Oct1, and examination of the consequences for transcription and DNA replication are important for understanding Oct1 function, and may also reveal a fundamental mechanism that regulates trans-acting factors during the cell cycle.

REFERENCES AND NOTES

1. A. Artishevsky *et al.*, *Mol. Cell. Biol.* **4**, 2364 (1984); N. Heintz *et al.*, *ibid.* **3**, 539 (1983); L. Hereford *et al.*, *Cell* **30**, 305 (1982); D. B. Sittman *et al.*, *Proc. Natl. Acad. Sci. U.S.A.* **80**, 1849 (1983); A. Artishevsky *et al.*, *Nature* **328**, 823 (1987).
2. S. Dalton and J. R. E. Wells, *EMBO J.* **7**, 49 (1988); *Mol. Cell. Biol.* **8**, 4576 (1988); P. Gallinari, F. LaBella, N. Heintz, *ibid.* **9**, 1566 (1989).
3. F. LaBella, P. Gallinari, J. McKinney, N. Heintz, *Genes Dev.* **3**, 982 (1989).
4. F. LaBella *et al.*, *ibid.* **2**, 32 (1988).
5. C. Fletcher *et al.*, *Cell* **51**, 773 (1987).
6. G. D. Johnson *et al.*, *Mol. Cell. Biol.* **10**, 982 (1990); S. Murphy *et al.*, *Cell* **59**, 1071 (1989); A. Pierani *et al.*, *Mol. Cell. Biol.* **110**, 6204 (1990); M. Tanaka *et al.*, *Genes Dev.* **2**, 1764 (1988).
7. H. L. Sive and R. G. Roeder, *Proc. Natl. Acad. Sci. U.S.A.* **83**, 6382 (1986).
8. R. P. Harvey, A. J. Robbins, J. R. E. Wells, *Nucleic Acids Res.* **10**, 7851 (1982); M. Perry, G. Thomsen, R. G. Roeder, *J. Mol. Biol.* **185**, 479 (1985).
9. E. A. O'Neil *et al.*, *Science* **241**, 1210 (1988).
10. P. Nurse and Y. Bissett, *Nature* **292**, 558 (1981); A. W. Murray and M. W. Kirschner, *Science* **246**, 614 (1989); L. H. Hartwell and T. A. Weinert, *ibid.*, p. 629; U. Surano *et al.*, *Cell* **65**, 145 (1991).
11. G. Draetta and D. Beach, *Cell* **54**, 17 (1988); G. Draetta, *Trends Biol. Sci.* **15**, 178 (1990); W. Krek and E. A. Nigg, *EMBO J.* **10**, 305 (1991); P. Nurse, *Nature* **344**, 503 (1990); P. Pondaven, L. Meijer, D. Beach, *Genes Dev.* **4**, 9 (1990).
12. M. Tanaka and W. Herr, *Cell* **60**, 375 (1990).
13. N. Segil, S. Roberts, N. Heintz, in preparation.
14. L. Gerace and G. Blobel, *Cell* **19**, 277 (1980).
15. S. Roberts and N. Segil, unpublished data.
16. R. Heald and F. McKeon, *Cell* **61**, 579 (1990); S. Moreno and P. Nurse, *ibid.*, p. 549.
17. L. Brizuela *et al.*, *EMBO J.* **6**, 3507 (1987).
18. C. Prives, *Cell* **61**, 735 (1990).
19. D. McVey *et al.*, *Nature* **341**, 503 (1989).
20. D. M. Virshup, M. G. Kauffman, T. J. Kelly, *EMBO J.* **8**, 3891 (1989).
21. HeLa D suspension cells (3×10^9) were fractionated by counterflow centrifugal elutriation (Beckman JE5.0 rotor) at 20°C with Joklik's modified Eagle medium to collect and wash the cells (*3*). Cells determined to be in G1 phase of the cell cycle by FACS analysis were immediately reinoculated into culture (5×10^5 cells per milliliter) in Joklik's medium that contained 5% bovine calf serum and grown at 37°C in suspension. An aliquot of synchronized cells was blocked in G1 with aphidicolin (5 μg/ml; Sigma) for 12 hours. An aliquot of synchronized cells was blocked in mitosis with nocodazole (40 ng/ml) by adding the drug at +8 hours when the cells were in S phase; cells were blocked for 12 hours. Washed cells were resuspended in dialyzed serum-supplemented (5%) methionine-free or phosphate-free Dulbecco's modified Eagle's medium (DMEM) for a 1-hour incubation before labeling. Cells were labeled for 1 hour at 37°C with [^{35}S]methionine (NEG-072) (500 to 700 μCi/ml) or [^{32}P]orthophosphate (NEX-053) (500 to 600 μCi/ml) in a volume of 2 ml (*24*). Cells were prepared for FACS analysis by adding an 800-μl aliquot of cells ($\sim 5 \times 10^5$) to 200 μl of a solution containing propidium iodide (10 μg) and Triton X-100 (5%) in H_2O. The cells were analyzed on a Becton Dickinson FACScan Flow Cytometer. Cells were prepared for mitotic index determination by a hypotonic lysis of a cell pellet (5×10^5) in H_2O (10 μl), followed by fixation with methanol (90 μl). DNA was stained with Hoechst 33258 (0.01 μg/ml). Whole cell extracts (WCE) from ^{32}P- and ^{35}S-labeled cells at 2×10^7 cells per milliliter were prepared in lysis buffer (1% NP-40, 0.5% deoxycholate, 0.4% SDS, 2 mM EDTA, 100 mM tris HCl, pH 7.6) (*17*). WCE from $\sim 5 \times 10^6$ cells were immunoprecipitated with 1 to 3 μl of the unpurified anti-Oct1 for 2 hours at 4°C. Immunoblots were prepared on nitrocellulose by electrotransfer (*24*). Aliquots of WCE (30 μg of protein) were diluted in SDS-PAGE sample buffer and fractionated on a 7.5% polyacrylamide gel. The gel was electroblotted overnight at 4°C, 25 V. Antibody was diluted 1:2000 and incubations were for 2 hours at room temperature. The signal was visualized with alkaline phosphatase ABC reagents (Vector Laboratories).
22. G. Pedrali-Noy *et al.*, *Nucleic Acids Res.* **8**, 377 (1980).
23. M. Nusse and H. J. Egner, *Cell Tissue Kinet.* **17**, 13 (1984); G. W. Zieve, D. Turnbull, J. M. Mullins, J. R. McIntosh, *Exp. Cell Res.* **126**, 397 (1980).
24. E. Harlow and D. Lane, *Antibodies: A Laboratory Manual* (Cold Spring Harbor Laboratory, Cold Spring Harbor, NY, 1988).
25. U. K. Laemmli, *Nature* **227**, 680 (1970).
26. P. H. O'Farrell, *J. Biol. Chem.* **250**, 4007 (1975); B. S. Dunbar, *Two-Dimensional Electrophoresis and Immunological Techniques* (Plenum, New York, 1987).
27. H. C. Hemmings, Jr., A. C. Nairn, P. Greengard, *J. Biol. Chem.* **259**, 14491 (1984).
28. Y. Ottaviano and L. Gerace, *J. Biol. Chem.* **260**, 624 (1985).
29. Synchronized HeLa cells were isolated by centrifugal elutriation (*3*). Mitotic cells were produced by inoculating an S phase population of elutriated cells into culture with nocodazole (5 ng/ml); after 12 hours the mitotic index was greater than 85%. WCE were prepared essentially as for nuclear extracts except that nuclei were not removed (*30*). The lysed cells were extracted with KCl (0.39 M) and β-mercaptoethanol (0.01 M) for 30 min. Extracts were cleared by centrifugation and supernatants were dialyzed to 100 mM KCl. Protein concentrations of extract were typically 10 to 20 mg/ml. To assay

mitotic kinase activity 5 μl of $p13^{suc1}$ or mock beads (*17*) were incubated at 4°C for 1 hour in the presence of 400 μg of WCE diluted in 2× bead buffer [bead buffer: 50 mM tris-Cl, pH 7.4, 5 mM NaF, 250 mM NaCl, 5 mM EDTA, 5 mM EGTA, 0.1% NP-40, 100 μM benzamidine, leupeptin (10 μg/ml), and aprotinin (10 μg/ml)]. Beads were washed twice with bead buffer and once with kinase buffer (25 mM MOPS, pH 7.2, 60 mM β-glycerophosphate, 5 mM EGTA, 15 mM $MgCl_2$, 1 mM dithiotheitol, 100 μM benzamidine) and incubated in 30 μl of kinase buffer that contained 1.6 μM adenosine triphosphate, 0.1 μM $^{32}P[\gamma ATP]$, 10 to 20 ng of Oct1, and 2.5 μg of histone H1. Phosphorylation of Oct1 was carried out for 10 min at 30°C.

30. N. Heintz and R. G. Roeder, *Proc. Natl. Acad. Sci. U.S.A.* **81**, 2713 (1983).

31. We thank J. C. Courvalin for the gracious gift of human lamin B antiserum; M. Thelen and A. Aderem for help with the phosphopeptide analyses; L. Dailey, R. Roeder, J. Darnell, and D. Baltimore for helpful discussion of the manuscript; and J. Newport for a $p13^{suc1}$ clone. Supported by NIH grant GM 13752 (N.S.), The Howard Hughes Medical Institute (N.H.), and NIH grant GM 32544.

30 April 1991; accepted 21 June 1991

Induction of Inflammatory Arthropathy Resembling Rheumatoid Arthritis in Mice Transgenic for HTLV-I

YOICHIRO IWAKURA,* MARIKO TOSU, EMI YOSHIDA, MASAFUMI TAKIGUCHI, KAZUTO SATO,† ISAO KITAJIMA,† KUSUKI NISHIOKA,† KAZUHIKO YAMAMOTO, TOSHIO TAKEDA, MASAKAZU HATANAKA, HIROAKI YAMAMOTO, TOYOZO SEKIGUCHI

Human T cell leukemia virus type-I (HTLV-I) is the etiologic agent of adult T cell leukemia and has also been suggested to be involved in other diseases such as chronic arthritis or myelopathy. To elucidate pathological roles of the virus in disease, transgenic mice were produced that carry the HTLV-I genome. At 2 to 3 months of age, many of the mice developed chronic arthritis resembling rheumatoid arthritis. Synovial and periarticular inflammation with articular erosion caused by invasion of granulation tissues were marked. These observations suggest a possibility that HTLV-I is one of the etiologic agents of chronic arthritis in humans.

VARIOUS ETIOLOGIC AGENTS INcluding viruses (*1, 2*), bacteria (*3–5*), and mycoplasmas (*6*) have been suggested as causes of rheumatoid arthritis in humans. However, so far no convincing evidence has been presented for a role of these agents in the disease. A high incidence of chronic arthritis has been reported in patients with HTLV-I–associated myelopathy, suggesting a possible involvement of HTLV-I in the disease (7). However, pathological roles of the virus, if any, remain obscure, because so far arthritogenic activity of the virus has not been shown. To examine the pathological effects of the virus on an animal, we produced lines of transgenic mice carrying the HTLV-I genome.

We constructed plasmid pHLX-I (8.8 kb), consisting of the 5′ long terminal repeat (LTR) 3′ end of *pol* [192 nucleotides (nts)]-*env-pX*-3′ LTR of HTLV-I, by replacing the Pvu II–Hind III fragment of pKCROHS (*8*) with the Sma I–Hind III fragment from the 5′ LTR clone of HTLV-I (pU3RU5) (Fig. 1B). We produced transgenic mice by injecting the Eco RI fragment (5.3 kb) containing the whole HTLV-I–derived sequence into fertilized mouse ova [(C3H/HeN × C57Bl/6J)F_2]. Both transgenic and nontransgenic siblings were kept in the same cages, and we checked pathological changes without knowing the genotype. Mice were cared for according to institutional guidelines and were kept in laminar-flow racks.

From a total of 960 ova injected, seven transgenic mice were obtained, and two mouse lines (T647 and T649) were established from these mice. Southern blot hybridization analysis of the tail DNA revealed that five to ten copies of the injected DNA were integrated intact into a single site of the host chromosome in a tandem fashion in both the T647 and T649 lines (*9*). Messenger RNA from the transgene could be detected in both line T647 and T649, but the level was more than 20 times higher in those mice from line T647 than in those from T649. Tissue specificity of the expression was rather broad; mRNA was strongly expressed in the brain, salivary gland, and joints and less intensely in various tissues, including the spleen, lung, eyeballs, muscle, and skin (Fig. 1A). Approximately equal amounts of mRNAs specific to the Env and pX proteins were detected in these tissues. The expression level of mRNA in the joints was approximately 1/2000 of that in MT-2 cells.

Swelling of the ankle with redness or swelling of the footpad near the ankle or all three symptoms were detected in 48 mice out of 141 transgenic T647 mice (Figs. 2 and 3A) and in 12 mice out of 126 transgenic T649 mice. In contrast, only one mouse out of 190 nontransgenic siblings demonstrated these changes, and none in unrelated transgenic mice that carry the human hepatitis B viral genome (104 mice) or the mouse interferon β gene (78 mice). The abnormality began to occur in female mice at age 2 to 3 months, and the proportion of affected mice increased thereafter until one year of age. At one year of age, almost half of the mice were affected. Onset in male mice was delayed 5 to 10 months, and the incidence was lower than that in female mice (10/47 and 38/94, respectively, in line T647 and 5/70 versus 7/56, respectively, in line T649). These abnormalities usually occurred in multiple ankle joints of a mouse. In some cases (5/141), swelling regressed after 1 to 4 months. The amounts of the mRNA specific to the transgene in the joints from affected mice were five to ten times higher than in those from apparently normal mice.

Joints from 15 affected transgenic mice were examined microscopically, and 12 of them were abnormal, whereas joints from 13 apparently normal transgenic mice showed no obvious changes except for slight degenerative changes of cartilage (4/13) and slight inflammatory cell infiltration in the synovial tissues (5/13). No abnormal changes were detected in joints from ten control nontransgenic mice. Histological observations of the affected joints are shown in Fig. 3. Erosion of the synovial bones and cartilage was marked in the ankle joint, and these tissues were replaced with pannus-like granulation tissues, which were composed of fibroblasts and small blood vessels accompanied by infiltration of lymphocytes, neutrophils, and macrophages (Fig. 3, B and C). Similar pathological changes were also observed in the joints of the toes (one in the four affected mice) and the knees (two in the four affected mice). In seven cases in the 13 affected mice, infiltration of inflammatory cells was found in the surrounding dermis, in the subcutaneous cells, and around the

Y. Iwakura, M. Tosu, E. Yoshida, M. Takiguchi, Institute of Medical Science, University of Tokyo, 4-6-1 Shirokanedai, Minato-ku, Tokyo 108, Japan.
K. Sato, I. Kitajima, K. Nishioka, Institute of Rheumatology, Tokyo Women's Medical College, Shinjuku-ku, Tokyo 163, Japan.
K. Yamamoto, Faculty of Medicine, University of Tokyo, Hongo, Bunkyo-ku, Tokyo 113, Japan.
T. Takeda, Chest Disease Research Institute, Kyoto University, Sakyo-ku, Kyoto 606, Japan.
M. Hatanaka, Institute for Virus Research, Kyoto University, Sakyo-ku, Kyoto 606, Japan.
H. Yamamoto and T. Sekiguchi, Kohno Clinical Medicine Research Institute, 3-3-7 Kitashinagawa, Shinagawa-ku, Tokyo 140, Japan.

*To whom correspondence should be addressed.
†Present address: Rheumatology Division, Institute of Medical Science, School of Medicine, St. Marriana University, Miyamac-ku, Kawasaki 213, Japan.